Adsorption of phenylglycine on copper: Density functional calculations

S. Blankenburg* and W. G. Schmidt
Theoretische Physik, Universität Paderborn, 33095 Paderborn, Germany
(Received 12 July 2006; revised manuscript received 16 August 2006; published 18 October 2006)

Density-functional theory in generalized gradient approximation is used to analyze the adsorption of phenylglycine on the Cu(110) surface. The molecule-substrate interaction is found to be dominated by covalent bonds. Intermolecular hydrogen bonds favor the formation of homochiral surface domains over heterochiral adsorption models for the (3×2) reconstruction.

DOI: 10.1103/PhysRevB.74.155419 PACS number(s): 68.43.−h, 73.20.−r, 82.45.Jn

I. INTRODUCTION

Self-organization of organic molecules appears as one of the most promising approaches to the further miniaturization of electronic devices. This so-called bottom-up approach contrasts with the exponentially increasing fabrication costs of further down scaling the lithographic processes for device manufacturing. The rich variety of living structures that are all based on different combinations of a few molecular building blocks, i.e., amino acids, proves the usefulness and robustness of the bottom-up approach for producing complex structures. However, we are only beginning to understand how the mechanisms of molecular recognition and self-assembly could be exploited for actual device production. In order to investigate the molecular self-organization, suitable model systems need to be found that allow for studying the molecular interactions reproducibly and with high accuracy. Surface adsorbed molecules are an obvious choice. They are accessible to sophisticated surface analysis tools such as scanning tunneling microscopy (STM) as well as electron diffraction techniques, infrared, and other optical spectroscopies. In this context, the physics and chemistry of organic molecules adsorbed on metals is intensively investigated.[1] The adsorption of adenine and phenylglycine on the Cu(110) surface is a particular impressive example for molecular self-organization: Scanning tunneling microscopy[2] (STM) images show that adenine adsorbed on Cu(110) forms ordered one-dimensional molecular chains that grow along the lateral $[\pm1,2]$ directions (given with respect to $[\bar{1}10]$ and $[001]$). The interaction of the adenine chains with phenylglycine leads to enantiomeric interactions. While coadsorption of *S*-phenylglycine leads to decorations of only those adenine chains that are oriented along the $[1, 2]$ direction in the surface plane, adsorption of *R*-phenylglycine on an adenine-treated Cu surface shows amino acid molecules now decorating chains aligned along $[-1,2]$.

In order to understand and predict such phenomena, it is required to explore the molecule-substrate interactions in detail. Recently it was shown that the adenine adsorption on Cu(110) is largely determined by mutual polarization and Coulomb interaction between the molecular amino group and the metal surface.[3] The interaction between *R*- and *S*-phenylglycine and Cu(110) has been studied using low energy electron diffraction[4] (LEED) and vibrational electron energy loss spectroscopy (EELS).[5] These studies show that at saturation coverage a well ordered, chiral overlayer structure forms. The commensurate $\begin{pmatrix}5&-3\\4&1\end{pmatrix}$ surface unit cell (*R*-phenylglycine) contains six admolecules. Upon annealing the surface, a (3×2) surface periodicity shows up. For the latter, a model with two molecules per unit cell was suggested.[4] While there are a number of first-principles calculations on glycine adsorbed on Cu(110), see, e.g., Refs. 6–8, we are not aware of any computational study on the adsorption of phenylglycine. The present work explores the adsorption of phenylglycine on Cu(110) using density-functional theory (DFT) with generalized gradient approximation (GGA).

II. COMPUTATIONAL METHOD

We use the Vienna ab initio Simulation Package (VASP) implementation[9] of DFT-GGA.[10] The electron-ion interaction is described by the projector-augmented wave (PAW) method,[11] which allows for an accurate treatment of the first-row elements as well as the Cu 3*d* electrons with a relatively moderate energy cutoff. We use a value of 340 eV throughout this work. The Brillouin zone integrations are performed using an $8\times8\times8$ Monkhorst-Pack mesh for bulk Cu and the Γ point for calculations of phenylglycine in the gas phase and surface calculations.

For bulk Cu we calculate an equilibrium lattice constant of 3.635 Å and a bulk modulus of 141 GPa in excellent agreement with the experimental values of 3.616 Å (Ref. 12) and 142 GPa,[13] respectively. Given the slight overestimation of the lattice constant and the underestimation of the bulk modulus typical for DFT-GGA, the agreement is excellent.

In order to determine the molecular ground state, we perform calculations for the experimentally observed phenylglycine conformers, see Fig. 1. Thereby the molecules were calculated within $30\times30\times60$ Å^3 supercells. Table I compares the energy differences calculated here with earlier

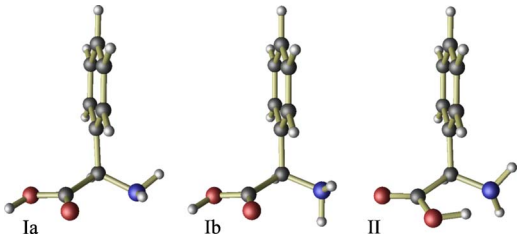

FIG. 1. (Color online) Low-energy conformers of phenylglycine. Notation according to Ref. 14.

TABLE I. Comparison of the relative energies (in eV) of the phenylglycine conformers shown in Fig. 1 obtained with MP2/6-311++$G(d,p)$ in Ref. 14 with the present calculations using DFT-GGA.

	Ia	Ib	II
ΔE^{MP2}	−0.017	0.000	−0.011
$\Delta E^{\mathrm{DFT\text{-}GGA}}$	−0.029	0.000	−0.079

MP2/6-311++$G(d,p)$ calculations.[14] While the MP2 calculations predicted the conformer Ia to be the most stable geometry, DFT-GGA favors conformer II. The maximum deviation of about 70 meV may be used as an estimate for the error bar for the present calculations.

To verify the accuracy of DFT-GGA in predicting molecular structures, we compare the available database values for the conformer Ib (Ref. 15) with the computed geometry parameters in Table II (see also Fig. 2). Obviously, the only significant deviation between the data calculated here, and Ref. 15 concerns the C—O bonding distance. This is related to the fact that the geometry of the latter refers to the dissociated species.

To model the Cu(110) surface, we use a periodically repeated slab. Each supercell consists of six atomic Cu layers plus the adsorbed phenylglycine molecule and a vacuum region above the phenylglycine equivalent in thickness to nine atomic Cu layers (≡11.57 Å). Six Cu layers are necessary to describe the relaxation of the Cu surface atoms correctly, i.e., to reproduce the measured trend of the layer spacing oscillations. The calculations are performed using the calculated Cu equilibrium lattice constant. The top five layers of the slab as well as the phenyglycine atoms are allowed to relax.

III. RESULTS AND DISCUSSION

A. Structure and energetics

Dosing $R(S)$-phenylglycine on Cu(110) at room temperature followed by annealing results in a $\begin{pmatrix} 5 & -(+)3 \\ 4 & +(-)1 \end{pmatrix}$ surface periodicity.[4] When mixtures of R- and S-phenylglycine are dosed on the clean Cu(110) surface, both $\begin{pmatrix} 5 & -3 \\ 4 & 1 \end{pmatrix}$ and $\begin{pmatrix} 5 & 3 \\ 4 & -1 \end{pmatrix}$ periodicities show up, suggesting the phase separation of the two enantiomers. Annealing the surface above 420 K causes a phase transition to a (3×2) periodicity. From the experiment it is not clear whether or not the phase separation of the enantiomers is maintained after annealing.

TABLE II. Phenylglycine (conformer Ib) bonding distances in Å calculated here in comparison with data from Ref. 15. For notation see Fig. 2.

Bonding atoms		Database	Present results
N	CA	1.452	1.463
CA	CB	1.496	1.521
CA	C	1.528	1.530
CB	CG1	1.388	1.401
CB	CG2	1.392	1.403
CG1	CD1	1.388	1.398
CG2	CD2	1.391	1.395
CD1	CE	1.389	1.397
CD2	CE	1.389	1.397
C	O	1.246	1.226
C	OXT	1.249	1.370

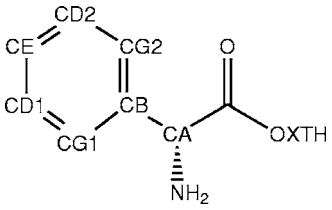

FIG. 2. Schematic phenylglycine structure for the notation of atoms.

To limit the complexity of the adsystem, we restrict our calculations to one and two phenylglycine molecules within a (3×2) surface periodicity, which we define as half and full monolayer (ML) coverage, respectively. From experiment it is known that hydrogen desorbs from the clean Cu surface at room temperature, see, e.g., Ref. 16. Therefore we focus in the present study mainly on the adsorption of the deprotonated species without considering the coadsorption of hydrogen in detail. The geometry optimization of a single admolecule on the Cu(110)(3×2) surface leads to the structure shown in the top part of Fig. 3. Thereby the conformer Ia with a deprotonated carboxyl group about 2.5 Å above the surface was used as starting configuration and a number of different initial positions were probed.

In order to map the potential-energy surface seen by phenylglycine on Cu(110), we fix the lateral positions of the down-most phenyl group carbon atom at a number of mesh points and allow for full relaxation of all other molecule and substrate atoms. The result is shown in the bottom part of Fig. 3. A pronounced corrugation of about one eV is predicted. The minimum energy position is reached when the molecular oxygens and the nitrogen atom are roughly above the substrate copper atoms.

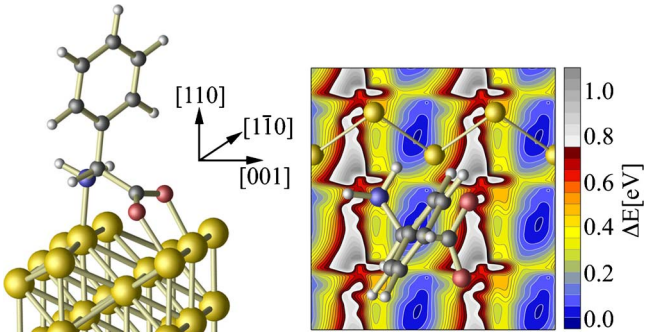

FIG. 3. (Color online) Left: Minimum-energy position of phenylglycine adsorbed on Cu(110). Right: Potential-energy surface seen by phenylglycine in bonding position above Cu(110). The legend shows the energy difference with respect to the minimum. The positions of the uppermost copper atoms are indicated in the upper part of the figure.

In Table III structural parameters of gas-phase phenylglycine (conformer Ia) are compared with those of the surface adsorbed molecule. Two main differences stand out: The C—OXT bond is shortened by about 0.09 Å and the C—O bond is elongated by about 0.06 Å upon adsorption. The former is indicative for a partial transition from a C—OXT single to a C═OXT double bond, related to the deprotonization. This also leads to a weakening of the C═O double bond. Structural changes occur also in the substrate: The copper atom underneath the molecular nitrogen moves out of the surface plane by 0.14 Å. The copper atoms underneath the oxygens move along the [001] direction by 0.09 Å (Cu_O) and 0.12 Å (Cu_{OXT}). In addition, they are lifted upwards by 0.17 and 0.10 Å, respectively.

The Cu—N distance of 2.07 Å is similar to the value of 2.04±0.02 Å determined by photoelectron diffraction for the respective bond of glycine adsorbed on Cu(110).[17] It is only slightly larger than the sum of the copper and nitrogen covalent radii of about 1.90 Å, indicating at least a partially covalent bonding. The same holds for O—Cu bonding. Here we calculate bond lengths of 1.99 Å and 2.00 Å that are almost equal to the respective value of 2.03±0.03 Å measured for glycine adsorbed on Cu(110).[17] Again, the calculated values are only slightly larger than the sum of the covalent radii of copper and oxygen of about 1.88 Å.

In agreement with the interpretation of the EELS results for the $\begin{pmatrix} 5 & -3 \\ 4 & 1 \end{pmatrix}$ adsorption structure,[5] the phenyl-group plane is close to the surface normal (tilted by 9.4°) and the carboxyl group is tilted with respect to the surface plane (by 27.4°). The tilt angle between the amino group and the surface amounts to 33.7°, smaller than found experimentally.[5]

The adsorption energy calculated from $E_{ad}=E_{ads/subs}-E_{subs}-E_{ads}+\frac{1}{2}E_{H_2}$ where E_{ads}, E_{subs}, $\frac{1}{2}E_{H_2}$, and $E_{ads/subs}$ refer to the energies of phenylglycine (conformer II), the relaxed copper surface, the hydrogen, and the total system, respectively, amounts to −1.35 eV. This appears to be relatively small, given the formation of three bonds. However, one also has to take into account the strain energy related to the molecular and substrate deformation upon bonding. For this we calculate a value of $E_{strain}=2.75$ eV, which increases the pure chemical bonding energy to $E_{bond}=-4.10$ eV. Due to the failure of DFT to account for van der Waals interaction, the bonding energy calculated here will probably underestimate the experiment by a few tenths of an eV.[18,19]

It is not possible to conclude directly on the strength of the bonding between the molecular amino and carboxyl group and the substrate from the calculated total adsorption energy. In order to obtain an estimate of the respective contributions to the bonding, the adsorption energies of ammonia (NH_3) and formate (HCOOH) on Cu(110) are calculated. The values obtained, $E_{ad,ammonia}=-0.89$ eV and $E_{ad,formate}=-0.84$ eV seem to indicate a roughly equal contribution of both functional groups to the total adsorption energy. A more realistic estimate, however, is probably obtained by calculating the adsorption energies of methylamine (CH_3NH_2) and acetate (CH_3COOH) on copper, taking the atomic positions from the phenylglycine adsorption. This results in $E_{ad,methylamine}=-0.96$ eV and $E_{ad,acetate}=-0.48$ eV. The sum of these values gets indeed close to the calculated adsorption energy of phenylglycine, indicating that the latter approach allows for a reliable estimate. It leads to the conclusion that the main contribution to the bonding is due to the interaction of the amino group with the surface. The smaller amount of energy released upon acetate adsorption is probably related to the larger strain: The acetate prefers an upright position on the surface which contrasts with the tilted geometry of adsorbed phenylglycine.

TABLE III. Comparison between bond lengths (in Å) of gas-phase and Cu(110) adsorbed phenylglycine. See Table II for notation.

Bonding atoms		Gas phase	Adsorbed
N	CA	1.463	1.490
CA	CB	1.521	1.513
CA	C	1.530	1.539
CB	CG1	1.401	1.402
CB	CG2	1.403	1.404
CG1	CD1	1.398	1.399
CG2	CD2	1.395	1.397
CD1	CE	1.397	1.395
CD2	CE	1.397	1.398
C	O	1.226	1.281
C	OXT	1.369	1.281

Next we investigate the influence of the substrate on the orientation of the phenyl group, which is not directly involved in the bonding to the Cu(110) surface. Figure 4 shows the energy profiles obtained by rotating the phenyl group of phenylglycine adsorbed in a (3×2) unit cell of Cu(110), in the same unit cell but without the substrate, and within a larger $20\times20\times30$ Å^3 supercell. These calculations allow for determining the influence of both the substrate and neighboring admolecules on the position of the phenyl group. The comparison of the curves shows that the substrate slightly enhances the corrugation of the rotation profile and that the molecule-molecule interaction does not favor phenyl groups oriented perpendicular to the carbon-carboxyl group bond. The alignment of the phenyl group concluded from the experiment for the $\begin{pmatrix} 5 & 3 \\ 4 & -1 \end{pmatrix}$ adsorption structure of about 75° coincides with an energy minimum in Fig. 4.

Next we turn to the case of two molecules adsorbed in a (3×2) surface unit cell, i.e., the monolayer adsorption supposedly described in Ref. 4. A large number of molecular starting configurations were probed and the rotational profiles of the phenyl groups were compared. In addition, the possible co-adsorption of the dissociated hydrogen was considered. The most stable heterochiral and a homochiral structures in the absence of coadsorbed hydrogen are shown in Fig. 5. We calculate adsorption energies of $E_{ad,hetero}=-1.29$ eV and $E_{ad,homo}=-1.35$ eV, respectively. Thus, compared to adsorption of single molecules, i.e., 0.5 ML, the adsorption energy decreases slightly for the heterochiral surface by $\Delta E_{ad,hetero}=0.06$ eV and remains constant for the homochiral surface, $\Delta E_{ad,homo}=0.0$ eV. Mainly two reasons may modify the adsorption energetics upon increasing the coverage: different adsorption sites with respect to the sub-

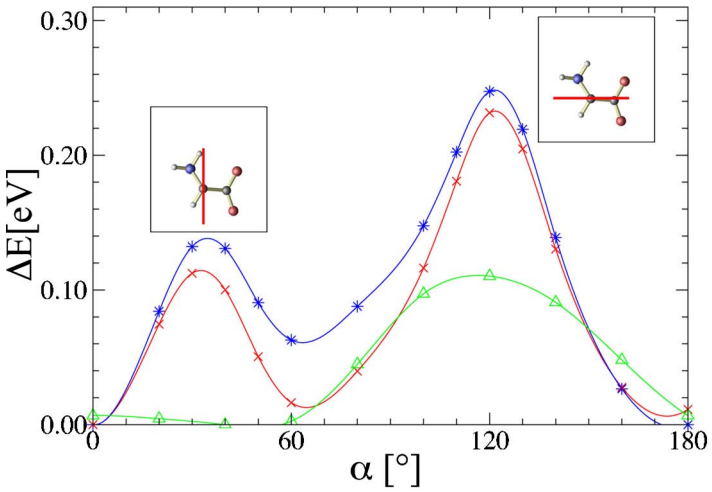

FIG. 4. (Color online) Energy rotation profile relative to the minimum energy of the phenyl group. Asterisks, crosses, and triangles refer to data obtained for phenylglycine adsorbed copper, gas-phase phenylglycine in the surface unit cell, and gas-phase phenylglycine in a $20\times20\times30$ Å^3 supercell. The solid lines are to guide the eye. The insets indicate the respective phenyl group orientation.

strate as well as possible intermolecular hydrogen bonds. In Fig. 5 we indicate potential hydrogen bonds provided they satisfy the following criteria: (i) $d(D-A)<3.00$ Å and (ii) $\angle(D-H\cdots A)>120°$ (D: donator, A: acceptor). Apart from these geometrical criteria, the formation of hydrogen bonds should lead to some charge polarization with respect to single adsorbed molecules. The respective charge-density differences

$$\Delta\rho(\mathbf{r}) = \rho_{\text{tot}}(\mathbf{r}) - \rho_{\text{ads}_1,\text{substr}}(\mathbf{r}) - \rho_{\text{ads}_2,\text{substr}}(\mathbf{r}) + \rho_{\text{substr}}(\mathbf{r}), \tag{1}$$

with ρ_{tot}, $\rho_{\text{ads}_i,\text{substr}}$, and ρ_{substr} being the densities of the adsystem with two phenylglycines, of the adsystem with one molecule, and of the clean substrate, respectively, are also shown in Fig. 5. At some potential hydrogen donors there is a clear electron accumulation. Based on this criterion, only two intermolecular hydrogen bonds form NH1—O and NH3—O for the homochiral and CH1—O and CH2—O for the heterochiral surface, respectively. This conclusion is also supported by analyzing the changes of the molecular CH and NH bonds upon adsorption, see Table IV. Obviously, the NH1 and NH3 bonds of the homochiral surface stretch upon adsorption, while the CH1 and CH2 bond of the heterochiral surface contract. We mention that—in contrast to the case of NH bonds—the CH bond contraction is indicative for a strengthening of the CH$\cdots$O hydrogen bond.[20] The values of Table IV indicate that the hydrogen bonds of the homochiral molecular network are stronger than those of the heterochiral surface, consistent with the trend of the adsorption energy discussed above.

In order to separate the molecular interaction energy due to hydrogen bonds from the adsorption energy changes resulting from different adsorption positions on the substrate,

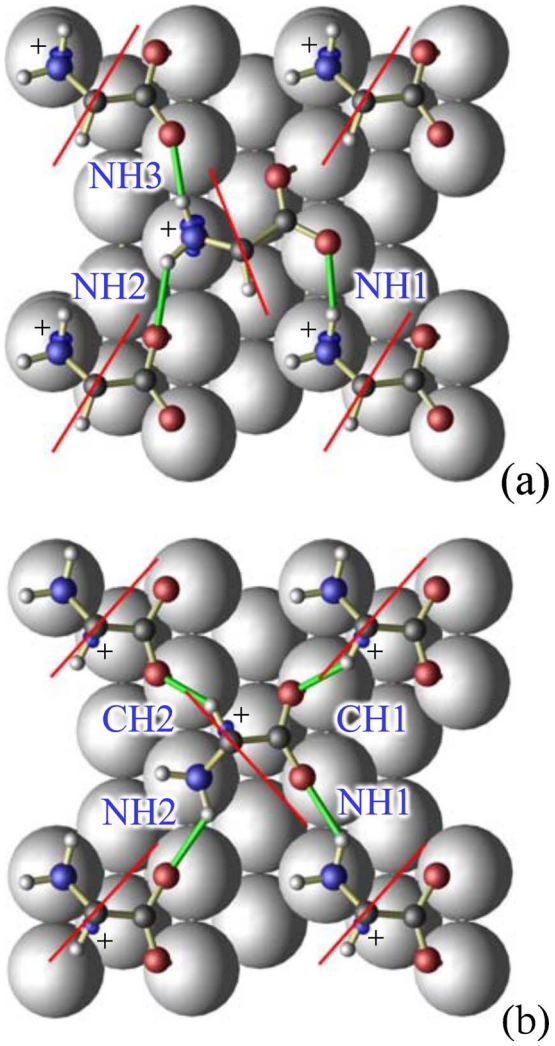

FIG. 5. (Color online) Two phenylgycines in adsorbed in a (3 $\times$2) surface unit cell in homochiral (a) and heterochiral (b) configuration. The phenyl-group orientations and possible hydrogen bonds (see text) are indicated with bars. There is also the total charge-density difference plotted with regions of electron accumulation (blue,+); isosurface value $0.04e/$Å^3.

we calculate $E_{\text{inter}}=E_{\text{tot}}-E_{\text{ads}_1,\text{substr}}-E_{\text{ads}_2,\text{substr}}+E_{\text{substr}}$ with E_{tot}, $E_{\text{ads}_i,\text{substr}}$, and E_{substr} being the energy of the adsystem with two phenylglycine molecules, the energy of the adsystem with one admolecule, and the energy of the clean substrate, respectively. It amounts to $E_{\text{inter,homo}}=-0.37$ eV and $E_{\text{inter,hetero}}=-0.09$ eV. The same calculations but without the

TABLE IV. NH and CH bond lengths (in Å) of surface adsorbed and gas-phase phenylglycine molecules, see Fig. 5 and text.

Bonding	Homochiral ML	Heterochiral ML	In gas phase
NH1	1.050	1.038	1.040
NH2	1.043	1.038	1.040
NH3	1.045		1.040
CH1		1.107	1.113
CH2		1.106	1.113

metallic substrate yield $E_{\text{inter,nosurf,homo}}=-0.49$ eV and $E_{\text{inter,nosurf,hetero}}=-0.40$ eV. These numbers show (i) that the homochiral monolayer is stabilized more by hydrogen bonds than the heterochiral monolayer and (ii) the weakening of intermolecular hydrogen bonds in the presence of the Cu surface. While the hydrogen-bond interactions are attractive for the formation of both homochiral and heterochiral surface phases, we find a repulsive contribution due to changes of the surface bonding site induced by the closer packing of the molecular overlayer. The energy loss amounts to 0.19 and 0.10 eV per molecule for the homochiral and heterochiral monolayer, respectively. However, the stronger intermolecular hydrogen bonds in the case of the homochiral surface overcompensate this effect.

In addition to the phenyglycine adsorption models discussed above, we also probe the energetics of configurations where hydrogen coadsorbes with phenylglycine or adsorbes exclusively on the surface. Thereby the adsorption of hydrogen in a pseudothreefold site ($\Theta=1$ ML) and in a long-bridge site[21] ($\Theta=\frac{1}{3}$ ML) is considered. Here one monolayer hydrogen adsorption is defined to correspond to the situation where all second row copper atoms are covered. In order to compare the energetics of these adsorption models, the thermodynamic grandcanonical potential[22]

$$\Omega(\{\mu_j\}) = G_{\text{surf}}(\{n_j\}) - \sum_j n_j\mu_j \approx E_{\text{surf}}(\{n_j\}) - \sum_j n_j\mu_j, \tag{2}$$

needs to be calculated. Here $G_{\text{surf}}(\{n_j\})$ is the surface free energy which we approximate by the total surface energy $E_{\text{surf}}(\{n_i\})$ at zero temperature, assuming similar entropy contributions for different adsorption configurations. The number of adsorbate molecules or atoms is represented by n_j. Figure 6 shows the resulting phase diagram in the dependence of the chemical potentials μ_{H} and μ_{pgl} that refer to molecular hydrogen and gas-phase phenyglycine at zero temperature. As can be seen, for zero temperature and in equilibrium with a hydrogen and phenylglycine reservoir, the homochiral ML with coadsorbed hydrogen is stable. If the hydrogen potential decreases to about −0.6 eV, corresponding to a partial pressure of about 10^{-12} Torr at room temperature, see Fig. 3 in Ref. 23, the H coadsorption is not favored anymore. Compared to the monolayer phenylglycine adsorption, the stability of the half-monolayer configuration is restricted to a very small region in the phase diagram.

B. Bonding mechanism

In order to analyze the bonding mechanism, we first consider the electron redistribution induced by the adsorption of single phenylglycine molecules on the Cu(110) surface. To quantify and analyze the charge transfer between molecule and substrate, we separate two subsystems by artificial planes as indicated in Fig. 7. The planes are placed halfway between the Cu and N or O atoms.

The charge-density difference of the relaxed adsorbate/substrate system $\rho_{\text{ads/subs}}$ with respect to the respective values for the the adsorbate ρ_{ads} and the substrate ρ_{subs}

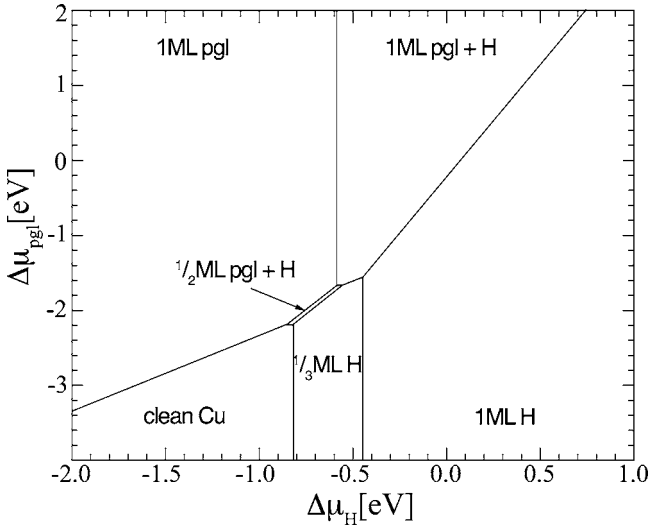

FIG. 6. Calculated phase diagram of the Cu(110) surface in dependence on the chemical potentials of hydrogen and phenylglycine (pgl) that are given with respect to molecular hydrogen and gas-phase phenylglycine at zero temperature.

$$\Delta\rho(\mathbf{r}) = \rho_{\text{ads/subs}}(\mathbf{r}) - \rho_{\text{ads}}(\mathbf{r}) - \rho_{\text{subs}}(\mathbf{r}) \tag{3}$$

allows for determining the total charge transfer

$$Q_{\text{I,II}} = -\int_{\text{I,II}} d\mathbf{r}\Delta\rho(\mathbf{r}) \tag{4}$$

and its average separation

$$d_i = -\frac{1}{Q_{\text{I}}}\int_{\text{I}} d\mathbf{r}x_i\Delta\rho(\mathbf{r}) + \frac{1}{Q_{\text{II}}}\int_{\text{II}} d\mathbf{r}x_i\Delta\rho(\mathbf{r}). \tag{5}$$

We calculate a net electron transfer from the substrate to the molecule of $|Q_{\text{I,II}}|=0.16e$. Q_{I} and Q_{II} are separated by $\mathbf{d}=(-0.02,-0.73,4.07)$ Å. This gives rise to an attractive Coulomb attraction of $E_{\text{mono-mono}}=-0.09$ eV. Using the same procedure as discussed above, we can calculate the adsorption induced dipoles in the subsystems I and II. They give

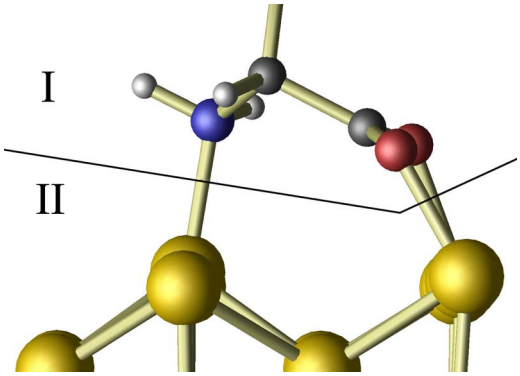

FIG. 7. (Color online) Dividing plane from subsystems I and II.

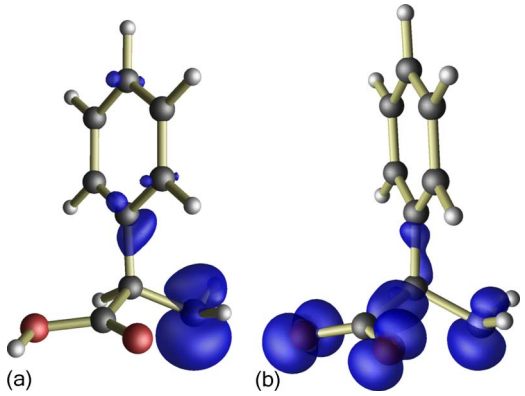

FIG. 8. (Color online) Charge density of the highest occupied molecule orbital (HOMO) for the (a) gas-phase molecule Ia and for (b) phenylglycine at the final bonding position. The isosurface marks a charge density of $0.1e/\text{Å}^3$.

rise to an repulsive interaction of $E_{\text{dipole-mono}}+E_{\text{mono-dipole}}+E_{\text{dipole-dipole}}=0.16-0.17+0.46=0.45$ eV. This means that the electrostatic polarization of adsorbate and substrate gives a net contribution to the bonding that is repulsive and small compared to the total adsorption energy. This is in marked contrast to the case of adenine adsorption on Cu(110), which was explained as determined mainly by mutual polarization and image forces.[3]

We now turn to investigate possible covalent interactions between molecule and substrate, starting with the amino-group metal bonding. In gas phase, the amino-group nitrogen is nearly tetrahedrally coordinated with angles ranging from 107.0° to 110.0° and one lone pair of electrons, indicative for an approximate sp^3 hybridization. This is consistent with the wave-function analysis giving the relative s and p contributions to the N localized occupied orbitals as $\chi_s=0.31$, $\chi_{p_x}=0.21$, $\chi_{p_y}=0.22$, $\chi_{p_z}=0.26$. The situation does not change much upon adsorption: The angles now range from 106.2° to 115.7° and the wave-function analysis yields $\chi_s=0.32$, $\chi_{p_x}=0.22$, $\chi_{p_y}=0.22$, $\chi_{p_z}=0.24$. The nitrogen lone pair of electrons, which directly points to the surface, is the highest occupied molecule orbital (HOMO), as shown in Fig. 8(a). It is thus susceptible to covalent interactions with the substrate. Upon adsorption of ammonia on Cu(110),[24] the N lone pair and an unoccupied molecular orbital hybridize with Cu $3d$ states. This leads to electron donation from the N lone pair to the substrate in conjunction with a back donation into an unoccupied hybrid orbital. In addition, there is a slight polarization of the Cu $4s$ states, that also contributes to the bonding. This picture largely holds also for the bonding between the phenylglycine amino group and the Cu surface. This is confirmed by the calculated charge-density difference, see Fig. 9. There is an electron accumulation in the center of the N—Cu bond, as expected for a covalent bond. In addition, there is a charge accumulation at molecular carbon atoms, indicative for electron back donation into unoccupied molecular orbitals.

The central carbon of the molecular carboxyl group in gas phase forms coordination angles between 111.9° and 124.8°, indicating some amount of sp^2 hybridization. This changes only slightly upon adsorption, where phenylgycine bonds in a deprotonated form with coordination angles ranging from 116.6° to 126.6°. Thus the oxygen p orbitals form σ and partially π bonds with carbon. In addition, we have p lone pairs that form the HOMO of phenylglycine in bonding position, shown in Fig. 8(b). In the case of formate adsorption on Cu(110), these O lone pairs form bonding and antibonding combinations with the metal d band.[1] There also occurs an interaction between metal valence states with previously unoccupied molecule orbitals.[1] Due to their spatial separation, the O p_π orbitals do not significantly contribute to the surface bonding. This is somewhat different in the present case of phenylglycine adsorption, where the O p_π orbitals are involved in the bonding. This becomes clear from the charge-density difference plot in Fig. 9. The electron redistribution involves oxygen p orbitals both in plane and out of plane with the Cu—O bonds. In addition to the charge accumulation in the center of the Cu—O bonds, there is a gain at the O atoms due to electron back donation from metal d to molecular states. Similarly to the case of formate adsorption,[1] there also occurs a charge accumulation at the CA—C bond (notation according to Fig. 2).

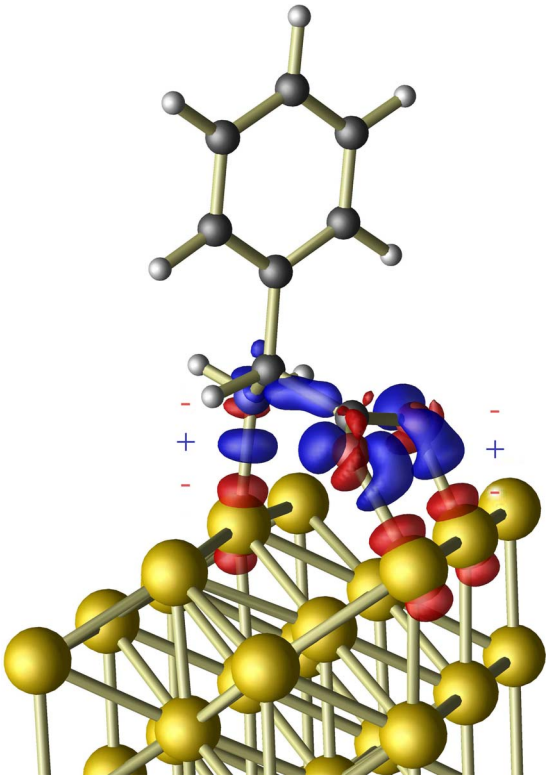

FIG. 9. (Color online) Total charge-density difference plot with regions of electron accumulation (blue, +) and depletion (red, −); isosurface value: $\pm 0.05e/\text{Å}^3$.

IV. CONCLUSIONS

The adsorption of phenylglycine on Cu(110) was calculated from *first principles*. Despite strong covalent interactions between molecule and substrate, the adsorption energy of about $E_{\text{ad}}=-1.3$ eV is moderate, due to the large strain

involved in the bond formation. In contrast to other cases of molecular adsorption on metals, we find the electrostatic interactions to be of minor importance. The comparison of structural models for the experimentally observed, phenylglycine induced (3×2) reconstruction shows a slight energetic preference of the homochiral phase. This is traced back to stronger intermolecular hydrogens bonds in comparison to heterochiral adsorption.

ACKNOWLEDGMENTS

We thank Neville Richardson for suggesting this work and helpful discussions. Martin Preuß and Andreas Hermann are acknowledged for technical assistance. The calculations were done using grants of computer time from the Paderborn Center for Parallel Computing (PC^2) and the Höchstleistungs-Rechenzentrum Stuttgart.

*Electronic address: blank@phys.upb.de

[1] A. Nilsson and L. G. M. Pettersson, Surf. Sci. Rep. **55**, 49 (2004).
[2] Q. Chen and N. V. Richardson, Nat. Mater. **2**, 324 (2003).
[3] M. Preuss, W. G. Schmidt, and F. Bechstedt, Phys. Rev. Lett. **94**, 236102 (2005).
[4] Q. Chen, C. W. Lee, D. J. Frankel, and N. V. Richardson, PhysChemComm **9**, 41 (1999).
[5] Q. Chen, D. J. Frankel, C. W. Lee, and N. V. Richardson, Chem. Phys. Lett. **349**, 167 (2001).
[6] M. Nyberg, J. Hasselström, O. Karis, N. Wassdahl, M. Weinelt, A. Nillson, and L. G. M. Pettersson, J. Chem. Phys. **112**, 5420 (2000).
[7] J. Hasselström, O. Karis, M. Nyber, L. G. M. Pettersson, M. Weinelt, N. Wassdahl, and A. Nilsson, J. Phys. Chem. B **104**, 11480 (2000).
[8] J. Hasselström, O. Karis, M. Weinelt, N. Wassdahl, A. Nilsson, M. Nyberg, L. G. M. Petterson, M. G. Samant, and J. Stöhr, Surf. Sci. **407**, 221 (1998).
[9] G. Kresse and J. Furthmüller, Comput. Mater. Sci. **6**, 15 (1996).
[10] J. P. Perdew, J. A. Chevary, S. H. Vosko, K. A. Jackson, M. R. Pederson, and D. J. Singh, and C. Fiolhais, Phys. Rev. B **46**, 6671 (1992).
[11] G. Kresse and D. Joubert, Phys. Rev. B **59**, 1758 (1999).
[12] *Landolt Börnstein* (Springer-Verlag, Berlin, 1998), Vol. 14a.
[13] G. Simmons and H. Wang, *Single Crystal Elastic Constants and Calculated Aggregate Properties: A Handbook* (MIT Press, Cambridge, 1971).
[14] M. E. Sanz, V. Cortijo, W. Caminati, J. C. Lpez, and J. L. Alonso, Chem.-Eur. J. **12**, 2564 (2006).
[15] A. Golovin, T. J. Oldfield, J. G. Tate, S. Velankar, G. J. Barton, H. Boutselakis, D. Dimitropoulos, J. Fillon, A. Hussain, J. M. C. Ionides, M. John, P. A. Keller, E. Krissinel, P. McNeil, A. Naim, R. Newman, A. Pajon, J. Pineda, A. Rachedi, J. Copeland, A. Sitnov, S. Sobhany, A. Suarez-Uruena, J. Swaminathan, M. Tagari, S. Tromm, W. Vranken, and K. Henrick, Nucleic Acids Res. **32**, D211 (2004).
[16] T. Genger, O. Hinrichsen, and M. Muhler, Catal. Lett. **59**, 137 (1999).
[17] N. A. Booth, D. P. Woodruff, O. Schaff, T. Gieel, R. Lindsay, P. Baumgärtel, and A. M. Bradshaw, Surf. Sci. **397**, 258 (1998).
[18] F. Ortmann, W. G. Schmidt, and F. Bechstedt, Phys. Rev. Lett. **95**, 186101 (2005).
[19] F. Ortmann, F. Bechstedt, and W. G. Schmidt, Phys. Rev. B **73**, 205101 (2006).
[20] Y. Gu, T. Kar, and S. Scheiner, J. Am. Chem. Soc. **121**, 9411 (1999).
[21] C. S. Bae, D. L. Freeman, J. D. Doll, G. Kresse, and J. Hafner, J. Chem. Phys. **113**, 6926 (2000).
[22] G-X Qian, R. M. Martin, and D. J. Chadi, Phys. Rev. B **38**, 7649 (1988).
[23] P. H. Hahn and W. G. Schmidt, Surf. Rev. Lett. **10**, 163 (2003).
[24] J. Hasselström, A. Föhlisch, O. Karis, N. Wassdahl, M. Weinelt, A. Nilsson, M. Nyberg, L. G. M. Pettersson, and J. Stöhr, J. Chem. Phys. **110**, 4880 (1999).